



PRIFYSGOL
BANGOR
UNIVERSITY

How does spatial variability of climate affect catchment streamflow predictions?,

Patil, S.D.; Wigington, P.J.; Leibowitz, S.G.; Sproles, E.A.; Comeleo, R.L.

Journal of Hydrology

DOI:

[10.1016/j.jhydrol.2014.05.017](https://doi.org/10.1016/j.jhydrol.2014.05.017)

Published: 17/05/2014

Peer reviewed version

[Cyswllt i'r cyhoeddiad / Link to publication](#)

Dyfyniad o'r fersiwn a gyhoeddwyd / Citation for published version (APA):

Patil, S. D., Wigington, P. J., Leibowitz, S. G., Sproles, E. A., & Comeleo, R. L. (2014). How does spatial variability of climate affect catchment streamflow predictions?, *Journal of Hydrology*, 517, 135–145. <https://doi.org/10.1016/j.jhydrol.2014.05.017>

Hawliau Cyffredinol / General rights

Copyright and moral rights for the publications made accessible in the public portal are retained by the authors and/or other copyright owners and it is a condition of accessing publications that users recognise and abide by the legal requirements associated with these rights.

- Users may download and print one copy of any publication from the public portal for the purpose of private study or research.
- You may not further distribute the material or use it for any profit-making activity or commercial gain
- You may freely distribute the URL identifying the publication in the public portal ?

Take down policy

Author's post-print must be released with a Creative Commons Attribution Non-Commercial No Derivatives License

Take down policy

If you believe that this document breaches copyright please contact us providing details, and we will remove access to the work immediately and investigate your claim.

NOTICE: This is the author's version of a work that was peer reviewed and accepted for publication in the Journal of Hydrology. Changes resulting from the publishing process, such as editing, corrections, structural formatting, and other quality control mechanisms may not be reflected in this document. A definitive version was subsequently published in JOURNAL OF HYDROLOGY, VOL 517, DOI <http://dx.doi.org/10.1016/j.jhydrol.2014.05.017>

How does spatial variability of climate affect catchment streamflow predictions?

Sopan D. Patil^{1,2}, Parker J. Wigington Jr.^{3,4}, Scott G. Leibowitz³, Eric A. Sproles^{1,5}, Randy L. Comeleo³

¹ ORISE, c/o U.S. Environmental Protection Agency,
200 SW 35th St., Corvallis, OR 97333, USA

² School of Environment, Natural Resources and Geography,
Bangor University,
Deiniol Road, Bangor, LL57 2UW, United Kingdom

³ Western Ecology Division,
National Health and Environmental Effects Research Laboratory,
U.S. Environmental Protection Agency,
200 SW 35th St., Corvallis, OR 97333, USA

⁴ Retired

⁵ Centro de Estudios Avanzados en Zonas Áridas

Universidad de La Serena

Raul Bitran s/n, La Serena, Chile

Submission to: Journal of Hydrology

Correspondence to: s.d.patil@bangor.ac.uk

Highlights:

- 1) We compare lumped and distributed hydrologic models at 41 catchments in northwest USA.
- 2) Distributed model performs better in catchments with low moisture homogeneity.
- 3) Spatial variability of precipitation phase is important in homogenous catchments.

1 **Abstract**

2 Spatial variability of climate can negatively affect catchment streamflow predictions if it is not
3 explicitly accounted for in hydrologic models. In this paper, we examine the changes in
4 streamflow predictability when a hydrologic model is run with spatially variable (distributed)
5 meteorological inputs instead of spatially uniform (lumped) meteorological inputs. Both lumped
6 and distributed versions of the EXP-HYDRO model are implemented at 41 meso-scale (500 –
7 5000 km²) catchments in the Pacific Northwest region of USA. We use two complementary
8 metrics of long-term spatial climate variability, moisture homogeneity index (I_M) and
9 temperature variability index (I_{TV}), to analyze the performance improvement with distributed
10 model. Results show that the distributed model performs better than the lumped model in 38 out
11 of 41 catchments, and noticeably better (>10% improvement) in 13 catchments. Furthermore,
12 spatial variability of moisture distribution alone is insufficient to explain the observed patterns of
13 model performance improvement. For catchments with low moisture homogeneity ($I_M < 80\%$),
14 I_M is a better predictor of model performance improvement than I_{TV} ; whereas for catchments
15 with high moisture homogeneity ($I_M > 80\%$), I_{TV} is a better predictor of performance
16 improvement than I_M . Based on the results, we conclude that: (1) catchments that have low
17 homogeneity of moisture distribution are the obvious candidates for using spatially distributed
18 meteorological inputs, and (2) catchments with a homogeneous moisture distribution benefit
19 from spatially distributed meteorological inputs if they also have high spatial variability of
20 precipitation phase (rain vs. snow).

21

22 **Keywords:** Hydrologic model, climate variability, streamflow, catchment

23 1 Introduction

24 Meteorological inputs such as precipitation, air temperature, and potential
25 evapotranspiration in spatially lumped hydrologic models consist of one-dimensional time series
26 data. These data are obtained either from a single meteorological station located within the
27 catchment [*Segond et al.*, 2007; *Vaze et al.*, 2011], from spatial interpolation of multiple
28 meteorological stations in the region [*Arnaud et al.*, 2002; *Chaubey et al.*, 1999; *Tobin et al.*,
29 2011], or from an areal mean of meteorological data grids that cover the catchment's drainage
30 area [*Koren et al.*, 1999; *Patil and Stieglitz*, 2014]. An important assumption in these models is
31 that the one-dimensional inputs are uniformly distributed over the entire catchment. Numerous
32 studies have shown that the quality of meteorological data used has a direct influence on the
33 quality of modeled streamflow predictions [*Andréassian et al.*, 2001; *Bárdossy and Das*, 2008;
34 *Faurès et al.*, 1995; *McMillan et al.*, 2011; *Obled et al.*, 1994; *Vaze et al.*, 2011]. *Andréassian et*
35 *al.* [2001] studied the impact of rain gage density on streamflow predictability at three
36 catchments in France and found that the performance of rainfall-runoff models was directly
37 proportional to the rain gage density used to generate the rainfall input. *Oudin et al.* [2006a]
38 studied the effect of random and systematic errors in climate input data on streamflow
39 predictions at 12 US catchments and found that random errors in rainfall series significantly
40 affect the model performance; however, systematic errors in potential evapotranspiration series
41 had greater impact on model performance than random errors. In Australia, *Vaze et al.* [2011]
42 observed improved performance in hydrologic models when rainfall estimates were obtained
43 from a gridded meteorological dataset compared to a single rain gage or a Thiessen weighted
44 average of multiple rain gages.

45 Regardless of the data preparation technique, a spatially uniform representation of
46 meteorological inputs has the potential to introduce significant uncertainty in catchments with
47 high spatial variability of climate, and can negatively affect streamflow predictability [*Bárdossy*
48 *and Das*, 2008; *Chaubey et al.*, 1999; *Moulin et al.*, 2009; *Shen et al.*, 2012]. Spatial variability
49 in rainfall can affect the estimation of hydrologic properties such as peak flow magnitude and
50 timing, stream flow volume, and soil moisture condition [*Arnaud et al.*, 2002; *Beven and*
51 *Hornberger*, 1982; *Krajewski et al.*, 1991; *Nicótina et al.*, 2008; *Tramblay et al.*, 2011]. On the
52 other hand, spatial variability in air temperature can affect the estimation of properties such as
53 snow cover extent, snow storage magnitude, and snowmelt timing [*Jefferson*, 2011; *Leibowitz et*
54 *al.*, 2012; *Nolin and Daly*, 2006; *Sproles et al.*, 2013]. Nonetheless, the degree to which spatial
55 variability of climate affects catchment streamflow predictions is not fully understood.

56 Hydrologic models that use spatially distributed meteorological data (henceforth referred
57 to as distributed models) are better equipped than those that use spatially uniform meteorological
58 data (henceforth referred to as lumped models) to handle the spatial variability of climate.
59 However, studies that have compared the lumped and distributed models provide a mixed picture
60 on the perceived advantage of distributed models. For instance, model comparisons using
61 theoretical approaches (e.g., virtual experiments) have typically been more favorable towards
62 distributed models [*Andréassian et al.*, 2004; *Krajewski et al.*, 1991; *Wilson et al.*, 1979; *Zhao et*
63 *al.*, 2013]. *Andréassian et al.* [2004] introduced the concept of chimera watersheds in which
64 multiple combinations of the data from real watersheds are used to create a large number of
65 virtual ‘chimera’ watersheds so that more heterogeneity can be obtained than is present in the
66 existing data. Using these chimera watersheds, *Andréassian et al.* [2004] showed that distributed
67 models provide much better simulation performance than lumped models. *Zhao et al.* [2013]

68 performed virtual experiments on 60 catchments in southeast Australia by systematically varying
69 the spatial variability of rainfall in each catchment (while still preserving the total rainfall
70 volume). The authors concluded that “for a given rainfall total, ignoring spatial rainfall
71 variability will result in underestimation of the total streamflow volume and overestimation of
72 evapotranspiration”. In contrast, studies that have used real catchment data show that in most
73 cases, only marginal improvements in streamflow predictions are obtained with distributed
74 models compared to lumped models [Boyle *et al.*, 2001; Das *et al.*, 2008; Refsgaard and
75 Knudsen, 1996; Vaze *et al.*, 2011]. Reed *et al.* [2004] summarized multiple results from the
76 Distributed Model Intercomparison (DMIP) initiative and concluded that in most of the DMIP
77 catchments, lumped models performed equally well or even slightly better than the distributed
78 models. Similar results were shown by Khakbaz *et al.* [2012] in the newer DMIP 2 study. Thus,
79 in spite of numerous studies comparing lumped and distributed models, we still cannot fully
80 differentiate the types of catchments that will truly benefit from the use of distributed models in
81 order to achieve improved streamflow predictability.

82 In this paper, our goal is to better understand the climatic conditions of catchments for
83 which a distributed model does (or does not) provide better streamflow predictions than a
84 lumped model. Both lumped and distributed versions of the Exponential Bucket Hydrologic
85 Model (EXP-HYDRO) [Patil and Stieglitz, 2014] are applied at 41 meso-scale catchments (500
86 – 5000 km²) in the Pacific Northwest region of USA. We begin with an *a priori* expectation
87 that, in the absence of any additional information, the distributed model will have the same
88 streamflow prediction capability as the lumped model at all catchments. For each catchment, we
89 then determine whether any improvement occurs with the use of the distributed model and
90 analyze this performance improvement within the context of long-term spatial climate variability

91 in the catchment. We characterize the spatial climate variability in all catchments by using two
92 different metrics, viz., moisture homogeneity index and temperature variability index.

93

94 **2 Study Area and Data**

95 Our study area is in the Pacific Northwest (PNW) region of USA and covers the states of
96 Oregon, Washington, and Idaho (Figure 1). Within these three states, we select 41 catchments
97 that satisfy the following two criteria: (1) they belong to either the HCDN [*Slack et al.*, 1993] or
98 GAGES [*Falcone et al.*, 2010] database of the U.S. Geological Survey (USGS), and (2) their
99 drainage areas are within the 500 to 5000 km² range. The selection from HCDN and GAGES
100 databases is done to ensure that the hydrologic regimes of the catchments are minimally
101 impacted by anthropogenic effects. The specified range limit of drainage areas is to ensure that
102 the catchments are large enough to detect spatial climate variability within them, but small
103 enough to ignore the delays in streamflow response due to channel network routing. The
104 drainage area of the catchments varies from 518 km² to 4956 km², with the median drainage area
105 of 865 km². The mean annual precipitation in the catchments varies from 540 mm to 3615 mm,
106 with the median value of 1251 mm. Of the 41 chosen catchments, 20 are located in Oregon, 7
107 are located in Washington, and 14 are located in Idaho (see Figure 1).

108 Climate of the PNW region is highly influenced by large scale atmospheric circulation
109 patterns caused by the presence of Pacific Ocean to the west and the subsequent interaction of
110 these patterns with the Cascade and Rocky Mountain ranges [*Salathé et al.*, 2008]. This
111 interaction creates a strong climate gradient in the west-to-east direction. The western parts of
112 the PNW, between the Pacific Ocean and the Cascade Mountains, experience high amounts of
113 rainfall and mild temperatures due to the maritime climate influence [*Wigington et al.*, 2013].

114 The eastern parts, between the Cascade and Rocky Mountains, are much drier because of the
115 rain-shadow effect of the Cascade Mountains and experience more extreme intra-annual
116 temperature differences. Roughly two-thirds of the precipitation in the PNW occurs during the
117 colder October to March period, while most of the region typically experiences dry summers.
118 Annual precipitation amounts and temperature are further influenced by the long term climate
119 trends caused by the El Niño Southern Oscillation (ENSO) and the Pacific Decadal Oscillation
120 (PDO) [Brown and Kipfmueller, 2011; Cayan, 1996]. Due to high elevations of the Cascades
121 and the Rockies, a significant amount of precipitation (much of it snow) is captured in the
122 region's mountains. As a result, the hydrology of major rivers in this region (e.g., Columbia,
123 Snake, and Willamette) is dominated by snow accumulation in the winter season and snowmelt
124 in the spring season [Hamlet and Lettenmaier, 1999; Regonda et al., 2005; Safeeq et al., 2013].

125 We use the daily streamflow data from USGS stream gages that are located at the outlet
126 of all 41 catchments. The time-span of the streamflow and meteorological input data is 20 years,
127 ranging from water year 1971 to 1990 (i.e., 1st October, 1970 to 30th September 1990). Daily
128 data of the meteorological inputs (precipitation and air temperature) is obtained from the gridded
129 observed meteorological dataset developed by Maurer et al. [2002]. This dataset has the spatial
130 resolution of 0.125 degrees (about 100 km² grid) and covers the entire continental United States.
131 Given that our smallest study catchment has a drainage area of 518 km², the ratio of the
132 meteorological grid resolution to basin size is less than 0.2 for all catchments. The methods used
133 to obtain the lumped and distributed versions of precipitation and air temperature inputs from the
134 gridded dataset for each catchment are described in Section 3.2. Daily potential
135 evapotranspiration inputs (both lumped and distributed version) are calculated directly from the
136 daily air temperature data using Hamon's formula [Hamon, 1963]. For calculation of the two

137 climate variability metrics at each catchment (see Section 3.3 for further details), we use the 30-
138 year (1971-2000) average values of precipitation, air temperature, and potential
139 evapotranspiration that are derived from the long-term data of Climate Source, Inc.
140 (http://www.climatesource.com/us/fact_sheets/fact_tmean_us_71b.html). This commercially
141 available data has a resolution of 400 m and covers the entire continental United States (see
142 *Wigington et al.* [2013] for details).

143

144 **3 Methods**

145 **3.1 Hydrologic model**

146 The EXP-HYDRO model was originally developed by *Patil and Stieglitz* [2014] as a
147 spatially lumped hydrologic model that operates at a daily time-step. In this paper, we have used
148 the original lumped version of the model as well as a modified version that explicitly accounts
149 for spatially distributed meteorological inputs (see section 3.2 for details). Below, we provide a
150 brief description of the model.

151 The EXP-HYDRO model conceptualizes a catchment as a bucket store that receives
152 water inputs in the form of liquid precipitation and snowmelt and has water outputs in the form
153 of evapotranspiration, subsurface runoff, and capacity-excess surface runoff (Figure 2). Daily
154 precipitation is first classified as either rainfall or snowfall, depending on the day's air
155 temperature. Snowfall accumulates separately into the snow accumulation bucket, whereas the
156 rainfall is input directly into the catchment bucket. Snowmelt from the snow accumulation
157 bucket is modeled using a thermal degree-day model, and the melt runoff generated is used as an
158 input to the catchment bucket. The amount of evapotranspiration in the catchment is calculated
159 as a fraction of potential evapotranspiration and depends on the ratio of actual water stored in the

160 catchment bucket on the given day to the catchment bucket's storage capacity. Subsurface
161 runoff depends on the amount of water stored in the catchment bucket and is calculated using a
162 TOPMODEL [Beven and Kirkby, 1979] type exponential equation. Capacity-excess surface
163 runoff occurs once the catchment bucket is filled to its capacity and there is still some excess
164 amount of water from the rainfall and snowmelt inputs. Catchment streamflow is calculated as
165 the sum of subsurface runoff and capacity-excess surface runoff. Detailed description of the
166 mathematical formulas of this model can be found in *Patil and Stieglitz* [2014] and *Patil et al.* [in
167 press].

168 There are six free calibration parameters in the EXP-HYDRO model: f , S_{\max} , Q_{\max} , D_f ,
169 T_{\max} , and T_{\min} . The parameter f (unit: 1/mm) controls the rate of decline in subsurface runoff
170 from the catchment bucket as its storage level fluctuates. S_{\max} (unit: mm) is the maximum
171 storage capacity of the catchment bucket. Q_{\max} (unit: mm/day) is the maximum subsurface
172 runoff that occurs when the catchment bucket is full. D_f (unit: mm/day/°C) is the thermal
173 degree-day factor that controls the rate of snowmelt from the snow bucket. T_{\max} (unit: °C) is the
174 air temperature above which snow starts melting, whereas T_{\min} (unit: °C) is the air temperature
175 below which precipitation falls as snow. We calibrate these parameters for each catchment with
176 50,000 Monte Carlo simulations [Vaché and McDonnell, 2006]. Parameter ranges used for the
177 random sampling of all six parameters are the same as those in *Patil and Stieglitz* [2014].
178 Modeled streamflow values from the first year are used for model spin-up. From the remaining
179 19 years of record, streamflow values of the first 9 years (water year 1972 to 1980) are used for
180 model calibration and those of the next 10 years (water year 1981 to 1990) are used for model
181 validation. Nash-Sutcliffe efficiency (NS) of square root transformed values of daily streamflow
182 (see *Oudin et al.* [2006b]) is used as the objective function for calibration:

183

$$NS = 1 - \frac{\sum_{i=1}^n (\sqrt{Q_{obs,i}} - \sqrt{Q_{pred,i}})^2}{\sum_{i=1}^n (\sqrt{Q_{obs,i}} - \sqrt{\bar{Q}_{obs}})^2} \quad (1)$$

184 where, $Q_{pred,i}$ and $Q_{obs,i}$ are the predicted and observed streamflow values ($L T^{-1}$) on the i^{th} day
 185 respectively, \bar{Q}_{obs} is the mean of all observed streamflow values ($L T^{-1}$), and n is the total
 186 number of days in the time series. We also use the water balance error (WBE) metric, in
 187 addition to NS, for the evaluation of model performance:

188

$$WBE = \frac{\sum_{i=1}^n Q_{pred,i} - \sum_{i=1}^n Q_{obs,i}}{\sum_{i=1}^n Q_{obs,i}} \times 100 \quad (2)$$

189 Following *Das et al.* [2008], the measure of model performance at a given catchment is obtained
 190 as an average of NS (and WBE) values from the calibration and validation model runs. The
 191 same calibration procedure is used for both lumped and distributed versions of the model.

192 **3.2 Spatially lumped and spatially distributed model configuration**

193 Each catchment is considered as a single areal unit for the lumped model and as a
 194 collection of multiple smaller areal units for the distributed model. Following *Wigington et al.*
 195 [2013], the smaller areal units within each catchment (henceforth referred to as landscape units)
 196 are delineated as first order sub-watersheds and incremental watersheds (Figure 3). For each
 197 catchment, we first extract the stream network from the USGS National Elevation Dataset's 30
 198 m DEM using a 25 km^2 minimum drainage area threshold for channel initiation. Landscape
 199 units are then delineated such that each unit consists of a single stream channel and a
 200 contributing local hillslope. As such, the landscape units developed here are analogous to the

201 Representative Elementary Watersheds (REWs) of *Reggiani et al.* [1999] or the assessment units
202 of *Wigington et al.* [2013].

203 For the lumped model, the daily precipitation and air temperature time series are obtained
204 by calculating an areal average of the values from meteorological grids that are either fully or
205 partially located within the catchment's drainage area. For the distributed model, the above
206 procedure is repeated at each individual landscape unit to obtain the spatially variable
207 precipitation and air temperature data in each catchment. Thus, if a particular catchment has 20
208 landscape units, then 20 distinct sets of the meteorological input data are created. To obtain
209 simulated stream flows, the lumped model is run in its original configuration with one-
210 dimensional meteorological input data [*Patil and Stieglitz, 2014*]. For the distributed
211 configuration, the EXP-HYDRO model is first run independently at each landscape unit (with
212 local meteorological input data). The streamflow output from all landscape units is then
213 aggregated to obtain catchment streamflow using the following formula:

$$214 \quad q_{catchment} = \frac{\sum_{i=1}^N q_i \cdot A_i}{\sum_{i=1}^N A_i} \quad (3)$$

215 where, $q_{catchment}$ is the streamflow at catchment outlet ($L T^{-1}$), N is the total number of landscape
216 units within the catchment, and q_i and A_i are the streamflow ($L T^{-1}$) and drainage area (L^2)
217 respectively of landscape unit i ($i = 1, 2, \dots, N$). It is important to note the following two
218 assumptions that are made in the distributed model: (1) channel network routing is ignored, i.e.,
219 the runoff generated from a landscape unit is assumed to reach the catchment outlet on the same
220 day, and (2) all six calibration parameters of the EXP-HYDRO model are assumed to be same in
221 every landscape unit within the catchment. Thus, the distributed EXP-HYDRO model presented

222 here is essentially the same as its lumped counterpart; the only difference being the spatially
 223 distributed meteorological inputs. Moreover, since the lumped and distributed models are
 224 calibrated separately at each catchment, the optimal parameter values are likely to be different
 225 for either configuration.

226 **3.3 Metrics of spatial climate variability**

227 We use two different metrics to quantify the spatial variability of climate within a
 228 catchment: (1) moisture homogeneity index, and (2) temperature variability index. Below, we
 229 describe how each of these indices is calculated for our study catchments.

230 For the moisture homogeneity index (I_M), we first classify the climate of each landscape
 231 unit based on the Feddema climate classification [Feddema, 2005]. This classification system
 232 uses a modified version of the Thornthwaite moisture index [Thornthwaite, 1948] as follows:

$$233 \quad I_f = \begin{cases} 1 - PET / P, & \text{if } P > PET \\ 0, & \text{if } P = PET \\ P / PET - 1, & \text{if } P < PET \end{cases} \quad (4)$$

234 where, I_f is the Feddema moisture index whose values vary between -1 and 1, and P and PET
 235 are the mean annual precipitation and potential evapotranspiration respectively (derived from the
 236 long-term data of Climate Source, Inc.; see Section 2). Following Wigington *et al.* [2013], we
 237 calculate the I_f values of each landscape unit and classify the units into one of the following six
 238 moisture classes: “V” (very wet, $I_f \geq 0.66$), “W” (wet, $0.66 > I_f \geq 0.33$), “M” (moist,
 239 $0.33 > I_f \geq 0$), “D” (dry, $0 > I_f \geq -0.33$), “S” (semi-arid, $-0.33 > I_f \geq -0.66$), and “A” (arid,
 240 $-0.66 > I_f$). The moisture homogeneity index I_M is then calculated as the percent areal
 241 coverage of the moisture class that has the maximum amount of area within the catchment.
 242 Thus, if a given catchment has completely homogeneous climate, all landscape units in that

243 catchment will belong to the same moisture class and the catchment will have an I_M value of
244 100%. Any value of I_M that is less than 100% is indicative of spatial variability of moisture
245 within the catchment.

246 For the temperature variability index (I_{TV}), we first obtain the mean annual temperature
247 T for each landscape unit (derived from the long-term data of Climate Source, Inc.; see Section
248 2). I_{TV} (unit: °C) is then calculated for each catchment with the following formula:

$$249 \quad I_{TV} = \max(T_1, T_2, \dots, T_N) - \min(T_1, T_2, \dots, T_N) \quad (5)$$

250 where, N is the total number of landscape units within the catchment.

251

252 **4 Results**

253 We first analyze the differences in simulation performance between the lumped and
254 distributed versions of the EXP-HYDRO model at all 41 study catchments. Figure 4a shows a
255 1:1 comparison of the NS values obtained with the lumped and distributed models. In most
256 catchments (38 out of 41) the distributed model has improved NS values than the lumped model,
257 although for 25 catchments the improvement is modest (< 10%). NS values for the lumped
258 model vary from 0.29 to 0.94, with a median value of 0.70. On the other hand, NS values for the
259 distributed model vary from 0.32 to 0.94, with a median value of 0.79. The percentage
260 improvement in NS values with the distributed model ranges from -0.12% to 49.67%, with a
261 median improvement of 6.63%. Out of the 41 catchments in total, 13 catchments show NS
262 improvement of greater than 10% with the distributed model. There are only three catchments
263 for which the distributed model has lower NS values than the lumped model, but with very small
264 amounts of deterioration (-0.12%, -0.11%, and -0.03%). Figure 4b shows a 1:1 comparison of
265 the WBE values obtained with the lumped and distributed models. For the majority of

266 catchments (with the exception of two outliers), the WBE values are located close to, and
267 scattered on both sides of, the 1:1 line. The two outlier catchments in Figure 4b are located in
268 the eastern drier region of Oregon. Both lumped and distributed models perform poorly at these
269 catchments ($NS < 0.4$). Therefore, we suspect that the big deviation of WBE values might be
270 arising from poor parameter identification at these catchments, rather than any physical reason.
271 The overall results from Figure 4 suggest that, unlike NS, there appears to be no systematic
272 difference between the lumped and distributed model in terms of the WBE metric.

273 Next, we examine the improvement in model performance achieved by the distributed
274 model within the context of long-term spatial climate variability in a catchment. For the purpose
275 of this analysis, we define model performance improvement as the % improvement in NS
276 obtained with the distributed model at each catchment. The two metrics of spatial climate
277 variability, I_M and I_{TV} , show considerable range among our study catchments. I_M varies from
278 38.1% to 100%, with a median value of 78.7%; whereas I_{TV} varies from 0.7 °C to 8.1 °C, with a
279 median value of 3.5 °C. Figures 5a and 5b show the relationship of % NS improvement with I_M
280 and I_{TV} , respectively. Both these relationships are also fit with a non-linear quadratic model to
281 determine how much of the variance in % NS improvement can be explained by each metric.
282 High performance improvement is observed for catchments with low I_M values (i.e., low
283 homogeneity of moisture distribution), and the amount of improvement declines with increasing
284 I_M value (Figure 5a). However, this declining pattern is observed only among catchments with
285 relatively low moisture homogeneity ($I_M < 80\%$). The relationship between % NS improvement
286 and I_M becomes scattered for the more homogeneous catchments ($I_M > 80\%$). The highest
287 variability of % NS improvement is observed in completely homogeneous catchments (

288 $I_M = 100\%$). For the metric I_{TV} , greater improvement in model performance is observed for
289 higher I_{TV} values (Figure 5b). Nonetheless, the relationship shows a high degree of scatter,
290 especially for higher values of I_{TV} . R^2 value of the non-linear quadratic fit (red dashed line in
291 Figures 5a and 5b) is 0.25 for the relationship of % NS improvement with I_M and 0.36 for the
292 relationship of % NS improvement with I_{TV} .

293 Since Figure 5a shows a noticeably different behavior for catchments with $I_M < 80\%$
294 than for those with $I_M > 80\%$, we segregate them into two distinct groups, henceforth referred to
295 as Group 1 ($I_M < 80\%$, $n = 21$) and Group 2 ($I_M > 80\%$, $n = 20$) catchments. Figure 6 shows
296 the location of both Group 1 and Group 2 catchments. Group 1 catchments are mostly located in
297 the central drier parts of the PNW; although there are a few along the Oregon Coast range and
298 the Rocky Mountains. Most of the Group 2 catchments are located in the wetter parts of the
299 PNW, along the western sides of the Cascade and Rocky Mountain ranges; a few are located
300 along the coastal mountains near the Pacific coast. Mean annual precipitation varies from 540
301 mm to 2340 mm (median = 935 mm) in Group 1 catchments, and from 812 mm to 3615 mm
302 (median = 1690 mm) in Group 2 catchments. We further examine the relationships of % NS
303 improvement with I_M and I_{TV} separately for each group. Figures 7a and 7b show the
304 relationship of % NS improvement with I_M and I_{TV} respectively for the Group 1 catchments. A
305 distinct and inversely proportional relationship is observed between % NS improvement and I_M
306 ($R^2 = 0.46$). On the other hand, a directly proportional but weaker ($R^2 = 0.21$) relationship is
307 observed between % NS improvement and I_{TV} . In sharp contrast, for Group 2 catchments
308 (Figures 7c and 7d), we find that virtually no relationship exists between % NS improvement and

309 I_M ($R^2 = 0.04$), whereas a strong non-linearly increasing relationship ($R^2 = 0.70$) exists between
310 % NS improvement and I_{TV} .

311

312 **5 Discussion**

313 Results show that the distributed version of EXP-HYDRO model performs better than its
314 lumped counterpart in 38 out of 41 catchments, and noticeably better (>10% NS improvement)
315 in 13 out of 41 catchments. This finding clearly demonstrates the importance of incorporating
316 spatially distributed meteorological inputs into hydrologic models, at least for certain types of
317 catchments. In a study similar to ours, *Vaze et al.* [2011] compared the lumped and distributed
318 versions of four hydrologic models at 240 catchments in southeast Australia. Contrary to our
319 results, they found that only marginal improvement occurred with distributed models, and most
320 of it in larger catchments (>1000 km²). However, *Vaze et al.* [2011] did not simulate snow
321 processes in their hydrologic models, and they also did not quantify the spatial climate variability
322 in their study catchments. Figure 8 shows the relationship of drainage area and % NS
323 improvement for our study catchments. This relationship is highly scattered and exhibits no
324 particular trend, which suggests that drainage area does not necessarily inform us about spatial
325 climate variability within a catchment.

326 Within the context of the PNW region (Figure 6), the two metrics of spatial climate
327 variability seem to provide complementary information. Specifically, the moisture homogeneity
328 index (I_M) represents the spatial variability of wetness, i.e., the competition of precipitation
329 input and evaporative demand, in a catchment. On the other hand, the temperature variability
330 index (I_{TV}) appears to represent the spatial variability of precipitation phase (rain vs. snow) in a
331 catchment. Figure 9 shows the relationship between I_{TV} and the lowest observed mean annual

332 temperature (amongst all landscape units) within a catchment. This relationship has a significant
333 declining trend ($R^2 = 0.59$, $p < 0.01$), and shows that catchments with high I_{TV} values tend to
334 have very low (near or below freezing) values of mean annual temperature in their coldest
335 landscape unit. This suggests that catchments with high I_{TV} values (i.e., high temperature
336 variability) are also likely to have high spatial variability of precipitation phase. Interestingly,
337 results show that neither I_M nor I_{TV} alone is sufficient to explain whether a particular catchment
338 will benefit from the use of a distributed model (Figures 5a and 5b). However, the combined use
339 of both these metrics provides a much better understanding of the types of catchments for which
340 the distributed model provides better streamflow predictions. A logical expectation would be
341 that catchments with low moisture homogeneity (low I_M) will have the largest % NS
342 improvement, and this improvement will reduce as we move towards catchments with more
343 homogeneous moisture distribution (high I_M). We do observe this trend, but only among the
344 Group 1 catchments (Figure 7a). Moreover, compared to I_M , I_{TV} has a weaker relationship
345 with % NS improvement for Group 1 catchments (Figure 7b). This suggests that for catchments
346 with relatively low moisture homogeneity, the spatial variability of wetness is a better indicator
347 of performance improvement with a distributed model than the spatial variability of precipitation
348 phase. A completely opposite behavior is observed for Group 2 catchments ($I_M > 80\%$). For
349 these catchments, I_M has virtually no explanatory power of % NS improvement (Figure 7c),
350 whereas I_{TV} has a substantially higher explanatory power (Figure 7d). This suggests that for
351 catchments with high moisture homogeneity, the spatial variability of precipitation phase is a
352 better indicator of performance improvement with a distributed model than the spatial variability
353 of wetness.

354 Figure 10 shows the thirteen catchments for which more than 10% NS improvement is
355 obtained with the distributed model. Of these, the seven Group 2 catchments with high wetness
356 homogeneity are located in wetter regions of the PNW (Olympic Peninsula, and the western
357 flanks of the Cascade and Rocky Mountains) where all parts of the catchment receive high
358 amounts of precipitation. However, the steep elevation gradients in these regions create
359 substantial spatial variability in air temperature [Jefferson, 2011; Leibowitz *et al.*, 2012; Nolin
360 and Daly, 2006]. This is reflected in the high I_{TV} values observed at most of these catchments
361 (Figure 7d). While spatially uniform meteorological inputs might provide good enough estimate
362 of precipitation amount in some cases, they are likely to miss the spatial variability of
363 precipitation phase. Use of lumped models in such catchments can lead to erroneous estimation
364 of the amount of snow accumulation and the timing of snowmelt. Thus, a spatially distributed
365 representation of meteorological inputs appears to be important in catchments where
366 heterogeneous precipitation phase is a significant factor (even if the same amount of
367 precipitation occurs in the rain and snow dominated areas). Capturing the spatial variability of
368 precipitation phase is even more critical in the wet mountainous areas of the PNW because most
369 climate change projections forecast a high vulnerability to the amount and the extent of snow
370 accumulation in those parts [Nolin and Daly, 2006; Regonda *et al.*, 2005; Salathé *et al.*, 2008;
371 Sproles *et al.*, 2013]. It is worth mentioning here that several hydrologic modeling studies have
372 also accounted for spatially variable precipitation phase by discretizing catchments in the vertical
373 dimension based on elevation bands [Abdulla and Lettenmaier, 1997; Hartman *et al.*, 1999;
374 Parajka and Blöschl, 2008]. Although beyond the scope of our study, it would be interesting to
375 compare how well the spatial variability of climate is represented when a catchment is
376 discretized in the vertical dimension (elevation bands) instead of horizontal dimension (sub-

377 catchments). The six Group 1 catchments in Figure 10 are located in the drier central parts of the
378 PNW. Catchments in this region typically contain rivers that are fed by a smaller headwater area
379 that receives most of the precipitation and flow downstream into a larger semi-arid landscape
380 [Wigington *et al.*, 2013]. Distributed models have an obvious advantage in these catchments
381 because a lumped representation of the meteorological inputs is likely to misestimate both
382 precipitation phase and magnitude.

383 A number of assumptions and simplifications were made in our methods that could
384 potentially influence the findings of this study. For the distributed EXP-HYDRO model, we
385 used the same parameter values in all landscape units. This simplification essentially ignores the
386 spatial variability of catchment properties such as land use, geology, and soil type, which can
387 play an important role in the filtering of spatially variable rainfall input. Numerous studies with
388 event scale hydrologic models have shown that a catchment's ability to dampen the rainfall
389 signal is an important indicator of whether a distributed model will perform better during a
390 spatially variable rainfall event [Arnaud *et al.*, 2002; Obled *et al.*, 1994; Segond *et al.*, 2007;
391 Smith *et al.*, 2004]. It is not clear though whether (and how) the heterogeneous catchment
392 properties will dampen the effects of spatially variable meteorological inputs for continuous
393 streamflow prediction. We also ignored channel network routing for the distributed EXP-
394 HYDRO model. The assumption here was that the runoff generated from all landscape units
395 reaches the catchment outlet on the same day. While we did choose catchments within a limited
396 range of drainage area (500 km² to 5000 km²) to mitigate the effects of this assumption, it is
397 possible that some catchments might benefit more than others by the use of distributed model
398 with explicit channel network routing. We used a gridded meteorological dataset [Maurer *et al.*,
399 2002] to generate both the lumped and distributed inputs for all catchments. The spatial

400 resolution and quality of this dataset has a huge influence on how well we can characterize the
401 spatial variability of meteorological inputs in our catchments. While the *Maurer et al.* [2002]
402 data has been used extensively in many hydrologic studies, it must be acknowledged that
403 precipitation estimates are usually poorer at high elevations and in regions with fewer
404 meteorological stations. The choice of using two specific climate variability metrics (I_M and
405 I_{TV}) also influenced the way in which our results were interpreted. For I_M , we were in many
406 ways building on the hydrologic classification work of *Wigington et al.* [2013] and chose the
407 areal dominance concept (of climate class) as a measure of homogeneity. Alternate metrics such
408 as Shannon's diversity index [*Shannon*, 1948] or the standard deviation of I_f could have served
409 a similar function, but we chose I_M due to the high physical realism of its numerical values. For
410 I_{TV} , our goal was to highlight the maximum extent of the spatial temperature contrast within
411 each catchment; especially because high elevation gradients in some parts the PNW create
412 distinct elevation divides for snow vs. rain type precipitation in the winter months. Alternate
413 metrics such as the standard deviation of air temperature could have also provided a function
414 similar to I_{TV} . We only used one type of model structure (EXP-HYDRO) to test the effects of
415 lumped and distributed meteorological inputs. While the use of a different model might provide
416 different quality of simulation performance, we think that similar findings (as of our study) are
417 likely to be obtained by using other commonly used hydrologic models. Moreover, studies with
418 multi-model assessments over a large number of catchments have shown that the geographic
419 patterns of hydrologic predictability tend to be more or less similar for models that include the
420 same hydrological processes [*Oudin et al.*, 2008; *Vaze et al.*, 2011].

421

422 6 Conclusions

423 In this paper, we compared the streamflow simulation performance of lumped and
424 distributed versions of the EXP-HYDRO model at 41 catchments in the Pacific Northwest region
425 of USA. Results showed that the distributed model performs better than the lumped model in
426 most (38 out of 41) catchments. Performance improvement using the distributed model (in
427 comparison to the lumped model) was further analyzed with respect to two metrics of spatial
428 climate variability in a catchment, viz., moisture homogeneity index (I_M) and temperature
429 variability index (I_{TV}). We found that for catchments with low moisture homogeneity (
430 $I_M < 80\%$), I_M was a better predictor of model performance improvement than I_{TV} . Such
431 catchments are more likely to be located in dry regions with small headwater areas that supply
432 most of the water. A completely opposite trend was observed among catchments with high
433 moisture homogeneity ($I_M > 80\%$), most of which were located in the wetter areas of the PNW.
434 Based on the results presented this study, we conclude that the use of spatially distributed
435 meteorological inputs in hydrologic models has the potential to substantially improve streamflow
436 predictions, at least for certain types of catchments. Catchments with highly variable moisture
437 distribution are the obvious candidates for using spatially distributed meteorological inputs in a
438 hydrologic model. On the other hand, homogeneously wet catchments can greatly benefit from
439 spatially distributed meteorological inputs if there is high spatial variability of precipitation
440 phase. Our assumption of spatially uniform model parameter values within a catchment ensured
441 that any improvement obtained with the distributed model was solely based on the spatially
442 distributed representation of meteorological inputs. However, this assumption will have to be
443 relaxed for future investigations of the effects of spatially variable land use, soil types, and/or
444 geology on catchment streamflow predictions.

445

446 **Acknowledgements**

447 We are thankful to J. Renée Brooks, Stacey Archfield, Marc Stieglitz, and two anonymous
448 reviewers for valuable comments and suggestions that have greatly improved the paper. The
449 first (Patil) and the fourth (Sproles) authors were supported by ORISE postdoctoral fellowship
450 for the duration of this study. The information in this document has been funded entirely by the
451 U.S. Environmental Protection Agency. This manuscript has been subjected to Agency review
452 and has been approved for publication. Mention of trade names or commercial products does not
453 constitute endorsement or recommendation for use.

454

455 **References**

456 Abdulla, F. A., and D. P. Lettenmaier (1997), Development of regional parameter estimation
457 equations for a macroscale hydrologic model, *Journal of Hydrology*, 197(1-4), 230-257,
458 doi: 10.1016/s0022-1694(96)03262-3.

459 Andréassian, V., C. Perrin, C. Michel, I. Usart-Sanchez, and J. Lavabre (2001), Impact of
460 imperfect rainfall knowledge on the efficiency and the parameters of watershed models,
461 *Journal of Hydrology*, 250(1-4), 206-223, doi: [http://dx.doi.org/10.1016/S0022-
462 1694\(01\)00437-1](http://dx.doi.org/10.1016/S0022-1694(01)00437-1).

463 Andréassian, V., A. Oddos, C. Michel, F. Anctil, C. Perrin, and C. Loumagne (2004), Impact of
464 spatial aggregation of inputs and parameters on the efficiency of rainfall-runoff models:
465 A theoretical study using chimera watersheds, *Water Resources Research*, 40(5),
466 W05209, doi: 10.1029/2003wr002854.

467 Arnaud, P., C. Bouvier, L. Cisneros, and R. Dominguez (2002), Influence of rainfall spatial
468 variability on flood prediction, *Journal of Hydrology*, 260(1–4), 216-230, doi:
469 [http://dx.doi.org/10.1016/S0022-1694\(01\)00611-4](http://dx.doi.org/10.1016/S0022-1694(01)00611-4).

470 Bárdossy, A., and T. Das (2008), Influence of rainfall observation network on model calibration
471 and application, *Hydrology and Earth System Sciences*, 12(1), 77-89, doi: 10.5194/hess-
472 12-77-2008.

473 Beven, K. J., and M. J. Kirkby (1979), A physically based, variable contributing area model of
474 basin hydrology / Un modèle à base physique de zone d'appel variable de l'hydrologie du
475 bassin versant, *Hydrological Sciences Bulletin*, 24(1), 43-69, doi:
476 10.1080/02626667909491834.

477 Beven, K. J., and G. M. Hornberger (1982), Assessing the effect of spatial pattern of
478 precipitation in modeling stream flow hydrographs, *JAWRA Journal of the American*
479 *Water Resources Association*, 18(5), 823-829, doi: 10.1111/j.1752-1688.1982.tb00078.x.

480 Boyle, D. P., H. V. Gupta, S. Sorooshian, V. Koren, Z. Zhang, and M. Smith (2001), Toward
481 improved streamflow forecasts: value of semidistributed modeling, *Water Resources*
482 *Research*, 37(11), 2749-2759, doi: 10.1029/2000wr000207.

483 Brown, D. P., and K. F. Kipfmueller (2011), Pacific Climate Forcing of Multidecadal Springtime
484 Minimum Temperature Variability in the Western United States, *Annals of the*
485 *Association of American Geographers*, 102(3), 521-530, doi:
486 10.1080/00045608.2011.627052.

487 Cayan, D. R. (1996), Interannual Climate Variability and Snowpack in the Western United
488 States, *Journal of Climate*, 9(5), 928-948, doi: 10.1175/1520-
489 0442(1996)009<0928:icvasi>2.0.co;2.

490 Chaubey, I., C. T. Haan, J. M. Salisbury, and S. Grunwald (1999), Quantifying model output
491 uncertainty due to spatial variability of rainfall, *JAWRA Journal of the American Water*
492 *Resources Association*, 35(5), 1113-1123, doi: 10.1111/j.1752-1688.1999.tb04198.x.

493 Das, T., A. Bárdossy, E. Zehe, and Y. He (2008), Comparison of conceptual model performance
494 using different representations of spatial variability, *Journal of Hydrology*, 356(1–2),
495 106-118, doi: <http://dx.doi.org/10.1016/j.jhydrol.2008.04.008>.

496 Falcone, J. A., D. M. Carlisle, D. M. Wolock, and M. R. Meador (2010), GAGES: A stream gage
497 database for evaluating natural and altered flow conditions in the conterminous United
498 States, *Ecology*, 91(2), 621-621, doi: 10.1890/09-0889.1.

499 Faurès, J.-M., D. C. Goodrich, D. A. Woolhiser, and S. Sorooshian (1995), Impact of small-scale
500 spatial rainfall variability on runoff modeling, *Journal of Hydrology*, 173(1–4), 309-326,
501 doi: [http://dx.doi.org/10.1016/0022-1694\(95\)02704-S](http://dx.doi.org/10.1016/0022-1694(95)02704-S).

502 Feddema, J. (2005), A Revised Thornthwaite-Type Global Climate Classification, *Physical*
503 *Geography*, 26(6), 442-466, doi: 10.2747/0272-3646.26.6.442.

504 Hamlet, A. F., and D. P. Lettenmaier (1999), Effects of Climate Change on Hydrology and
505 Water Resources in the Columbia River Basin, *JAWRA Journal of the American Water*
506 *Resources Association*, 35(6), 1597-1623, doi: 10.1111/j.1752-1688.1999.tb04240.x.

507 Hamon, W. R. (1963), Computation of direct runoff amounts from storm rainfall, *Int. Assoc. Sci.*
508 *Hydrol. Publ*, 63, 52–62, doi.

509 Hartman, M. D., J. S. Baron, R. B. Lammers, D. W. Cline, L. E. Band, G. E. Liston, and C.
510 Tague (1999), Simulations of snow distribution and hydrology in a mountain basin,
511 *Water Resources Research*, 35(5), 1587-1603, doi: 10.1029/1998wr900096.

512 Jefferson, A. J. (2011), Seasonal versus transient snow and the elevation dependence of climate
513 sensitivity in maritime mountainous regions, *Geophysical Research Letters*, 38(16),
514 L16402, doi: 10.1029/2011gl048346.

515 Khakbaz, B., B. Imam, K. Hsu, and S. Sorooshian (2012), From lumped to distributed via semi-
516 distributed: Calibration strategies for semi-distributed hydrologic models, *Journal of*
517 *Hydrology*, 418–419, 61-77, doi: <http://dx.doi.org/10.1016/j.jhydrol.2009.02.021>.

518 Koren, V. I., B. D. Finnerty, J. C. Schaake, M. B. Smith, D. J. Seo, and Q. Y. Duan (1999), Scale
519 dependencies of hydrologic models to spatial variability of precipitation, *Journal of*
520 *Hydrology*, 217(3–4), 285-302, doi: [http://dx.doi.org/10.1016/S0022-1694\(98\)00231-5](http://dx.doi.org/10.1016/S0022-1694(98)00231-5).

521 Krajewski, W. F., V. Lakshmi, K. P. Georgakakos, and S. C. Jain (1991), A Monte Carlo Study
522 of rainfall sampling effect on a distributed catchment model, *Water Resources Research*,
523 27(1), 119-128, doi: 10.1029/90wr01977.

524 Leibowitz, S. G., P. J. Wigington Jr, R. L. Comeleo, and J. L. Ebersole (2012), A temperature-
525 precipitation-based model of thirty-year mean snowpack accumulation and melt in
526 Oregon, USA, *Hydrological Processes*, 26(5), 741-759, doi: 10.1002/hyp.8176.

527 Maurer, E. P., A. W. Wood, J. C. Adam, D. P. Lettenmaier, and B. Nijssen (2002), A Long-Term
528 Hydrologically Based Dataset of Land Surface Fluxes and States for the Conterminous
529 United States, *Journal of Climate*, 15(22), 3237-3251, doi: 10.1175/1520-
530 0442(2002)015<3237:althbd>2.0.co;2.

531 McMillan, H., B. Jackson, M. Clark, D. Kavetski, and R. Woods (2011), Rainfall uncertainty in
532 hydrological modelling: An evaluation of multiplicative error models, *Journal of*
533 *Hydrology*, 400(1–2), 83-94, doi: <http://dx.doi.org/10.1016/j.jhydrol.2011.01.026>.

534 Moulin, L., E. Gaume, and C. Obled (2009), Uncertainties on mean areal precipitation:
535 assessment and impact on streamflow simulations, *Hydrology and Earth System Sciences*,
536 *13*(2), 99-114, doi: 10.5194/hess-13-99-2009.

537 Nicótina, L., E. Alessi Celegon, A. Rinaldo, and M. Marani (2008), On the impact of rainfall
538 patterns on the hydrologic response, *Water Resources Research*, *44*(12), W12401, doi:
539 10.1029/2007wr006654.

540 Nolin, A. W., and C. Daly (2006), Mapping “At Risk” Snow in the Pacific Northwest, *Journal of*
541 *Hydrometeorology*, *7*(5), 1164-1171, doi: 10.1175/jhm543.1.

542 Obled, C., J. Wendling, and K. Beven (1994), The sensitivity of hydrological models to spatial
543 rainfall patterns: an evaluation using observed data, *Journal of Hydrology*, *159*(1–4),
544 305-333, doi: [http://dx.doi.org/10.1016/0022-1694\(94\)90263-1](http://dx.doi.org/10.1016/0022-1694(94)90263-1).

545 Oudin, L., C. Perrin, T. Mathevet, V. Andréassian, and C. Michel (2006a), Impact of biased and
546 randomly corrupted inputs on the efficiency and the parameters of watershed models,
547 *Journal of Hydrology*, *320*(1–2), 62-83, doi:
548 <http://dx.doi.org/10.1016/j.jhydrol.2005.07.016>.

549 Oudin, L., V. Andréassian, T. Mathevet, C. Perrin, and C. Michel (2006b), Dynamic averaging
550 of rainfall-runoff model simulations from complementary model parameterizations,
551 *Water Resources Research*, *42*(7), W07410, doi: 10.1029/2005wr004636.

552 Oudin, L., V. Andréassian, C. Perrin, C. Michel, and N. Le Moine (2008), Spatial proximity,
553 physical similarity, regression and ungaged catchments: A comparison of regionalization
554 approaches based on 913 French catchments, *Water Resources Research*, *44*(3), W03413,
555 doi: 10.1029/2007wr006240.

556 Parajka, J., and G. Blöschl (2008), The value of MODIS snow cover data in validating and
557 calibrating conceptual hydrologic models, *Journal of Hydrology*, 358(3-4), 240-258, doi:
558 <http://dx.doi.org/10.1016/j.jhydrol.2008.06.006>.

559 Patil, S., and M. Stieglitz (2014), Modelling daily streamflow at ungauged catchments: what
560 information is necessary?, *Hydrological Processes*, 28(3), 1159-1169, doi:
561 10.1002/hyp.9660.

562 Patil, S. D., P. J. Wigington Jr, S. G. Leibowitz, and R. L. Comeleo (in press), Use of hydrologic
563 landscape classification to diagnose streamflow predictability in Oregon, *JAWRA Journal*
564 *of the American Water Resources Association*, doi: 10.1111/jawr.12143.

565 Reed, S., V. Koren, M. Smith, Z. Zhang, F. Moreda, D.-J. Seo, and a. Dmip Participants (2004),
566 Overall distributed model intercomparison project results, *Journal of Hydrology*, 298(1-
567 4), 27-60, doi: <http://dx.doi.org/10.1016/j.jhydrol.2004.03.031>.

568 Refsgaard, J. C., and J. Knudsen (1996), Operational Validation and Intercomparison of
569 Different Types of Hydrological Models, *Water Resources Research*, 32(7), 2189-2202,
570 doi: 10.1029/96wr00896.

571 Reggiani, P., S. M. Hassanizadeh, M. Sivapalan, and W. G. Gray (1999), A unifying framework
572 for watershed thermodynamics: constitutive relationships, *Advances in Water Resources*,
573 23(1), 15-39, doi: 10.1016/s0309-1708(99)00005-6.

574 Regonda, S. K., B. Rajagopalan, M. Clark, and J. Pitlick (2005), Seasonal Cycle Shifts in
575 Hydroclimatology over the Western United States, *Journal of Climate*, 18(2), 372-384,
576 doi: 10.1175/jcli-3272.1.

577 Safeeq, M., G. E. Grant, S. L. Lewis, and C. L. Tague (2013), Coupling snowpack and
578 groundwater dynamics to interpret historical streamflow trends in the western United
579 States, *Hydrological Processes*, 27(5), 655-668, doi: 10.1002/hyp.9628.

580 Salathé, E. P., R. Steed, C. F. Mass, and P. H. Zahn (2008), A High-Resolution Climate Model
581 for the U.S. Pacific Northwest: Mesoscale Feedbacks and Local Responses to Climate
582 Change, *Journal of Climate*, 21(21), 5708-5726, doi: 10.1175/2008jcli2090.1.

583 Segond, M.-L., H. S. Wheater, and C. Onof (2007), The significance of spatial rainfall
584 representation for flood runoff estimation: A numerical evaluation based on the Lee
585 catchment, UK, *Journal of Hydrology*, 347(1-2), 116-131, doi:
586 <http://dx.doi.org/10.1016/j.jhydrol.2007.09.040>.

587 Shannon, C. E. (1948), A mathematical theory of communication, *Bell System Technical*
588 *Journal*, 27, 623-656, doi.

589 Shen, Z., L. Chen, Q. Liao, R. Liu, and Q. Hong (2012), Impact of spatial rainfall variability on
590 hydrology and nonpoint source pollution modeling, *Journal of Hydrology*, 472-473(0),
591 205-215, doi: <http://dx.doi.org/10.1016/j.jhydrol.2012.09.019>.

592 Slack, J. R., A. Lumb, and J. M. Landwehr (1993), Hydro-Climatic Data Network (HCDN)
593 Streamflow Data Set, 1874-1988: *USGS Water-Resources Investigations Report 93-4076*,
594 U.S. Geological Survey, Reston, VA.

595 Smith, M. B., V. I. Koren, Z. Zhang, S. M. Reed, J.-J. Pan, and F. Moreda (2004), Runoff
596 response to spatial variability in precipitation: an analysis of observed data, *Journal of*
597 *Hydrology*, 298(1-4), 267-286, doi: <http://dx.doi.org/10.1016/j.jhydrol.2004.03.039>.

598 Sproles, E., A. Nolin, K. Rittger, and T. Painter (2013), Climate change impacts on maritime
599 mountain snowpack in the Oregon Cascades, *Hydrol. Earth Syst. Sci.*, 17(7), 2581-2597,
600 doi: 10.5194/hess-17-2581-2013.

601 Thornthwaite, C. W. (1948), An approach toward a rational classification of climate,
602 *Geographical review*, 38(1), 55-94, doi.

603 Tobin, C., L. Nicotina, M. B. Parlange, A. Berne, and A. Rinaldo (2011), Improved interpolation
604 of meteorological forcings for hydrologic applications in a Swiss Alpine region, *Journal*
605 *of Hydrology*, 401(1–2), 77-89, doi: <http://dx.doi.org/10.1016/j.jhydrol.2011.02.010>.

606 Trambly, Y., C. Bouvier, P. A. Ayrat, and A. Marchandise (2011), Impact of rainfall spatial
607 distribution on rainfall-runoff modelling efficiency and initial soil moisture conditions
608 estimation, *Nat. Hazards Earth Syst. Sci.*, 11(1), 157-170, doi: 10.5194/nhess-11-157-
609 2011.

610 Vaché, K. B., and J. J. McDonnell (2006), A process-based rejectionist framework for evaluating
611 catchment runoff model structure, *Water Resources Research*, 42(2), W02409, doi:
612 10.1029/2005wr004247.

613 Vaze, J., D. A. Post, F. H. S. Chiew, J. M. Perraud, J. Teng, and N. R. Viney (2011), Conceptual
614 Rainfall–Runoff Model Performance with Different Spatial Rainfall Inputs, *Journal of*
615 *Hydrometeorology*, 12(5), 1100-1112, doi: 10.1175/2011jhm1340.1.

616 Wigington, P. J., S. G. Leibowitz, R. L. Comeleo, and J. L. Ebersole (2013), Oregon Hydrologic
617 Landscapes: A Classification Framework, *JAWRA Journal of the American Water*
618 *Resources Association*, 49(1), 163-182, doi: 10.1111/jawr.12009.

619 Wilson, C. B., J. B. Valdes, and I. Rodriguez-Iturbe (1979), On the influence of the spatial
620 distribution of rainfall on storm runoff, *Water Resources Research*, 15(2), 321-328, doi:
621 10.1029/WR015i002p00321.

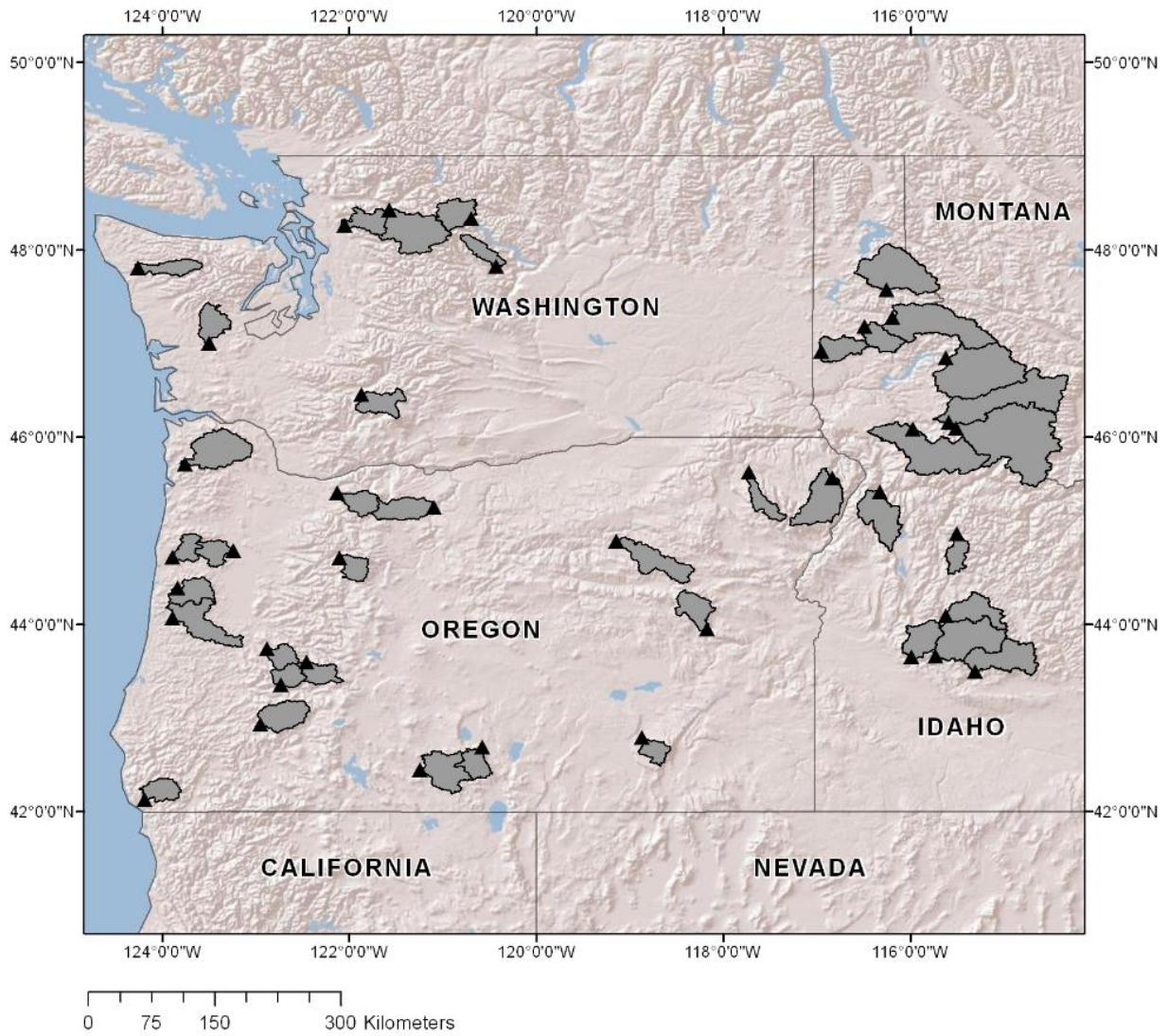
622 Zhao, F., L. Zhang, F. H. S. Chiew, J. Vaze, and L. Cheng (2013), The effect of spatial rainfall
623 variability on water balance modelling for south-eastern Australian catchments, *Journal*
624 *of Hydrology*, 493(0), 16-29, doi: <http://dx.doi.org/10.1016/j.jhydrol.2013.04.028>.

625

626

627

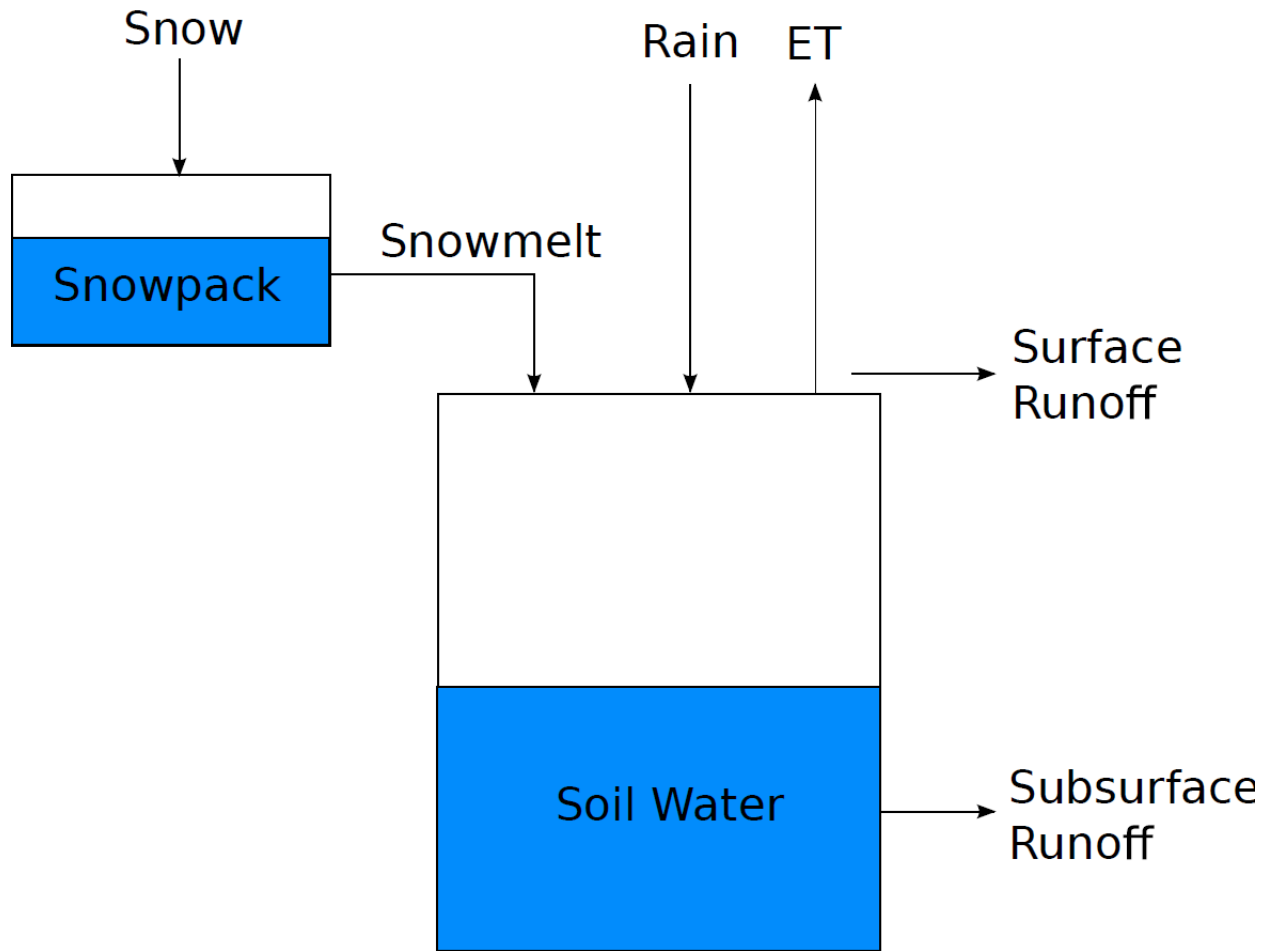
628 **Figures:**



629

630 **Figure 1:** Location of the 41 study catchments. Black triangles are the catchment outlets,
631 whereas gray regions are the drainage areas.

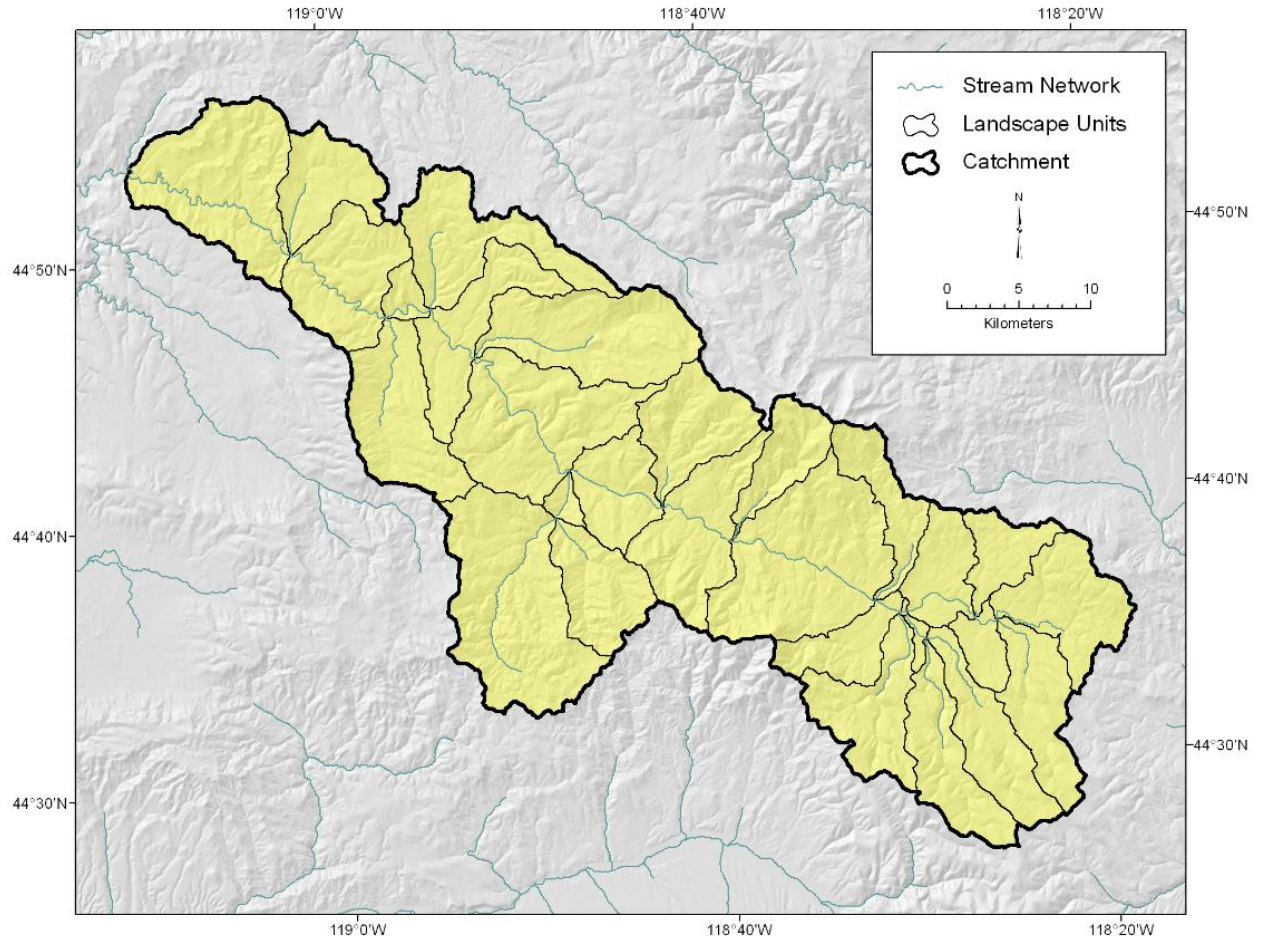
632



633

634 **Figure 2:** Schematic representation of the EXP-HYDRO model.

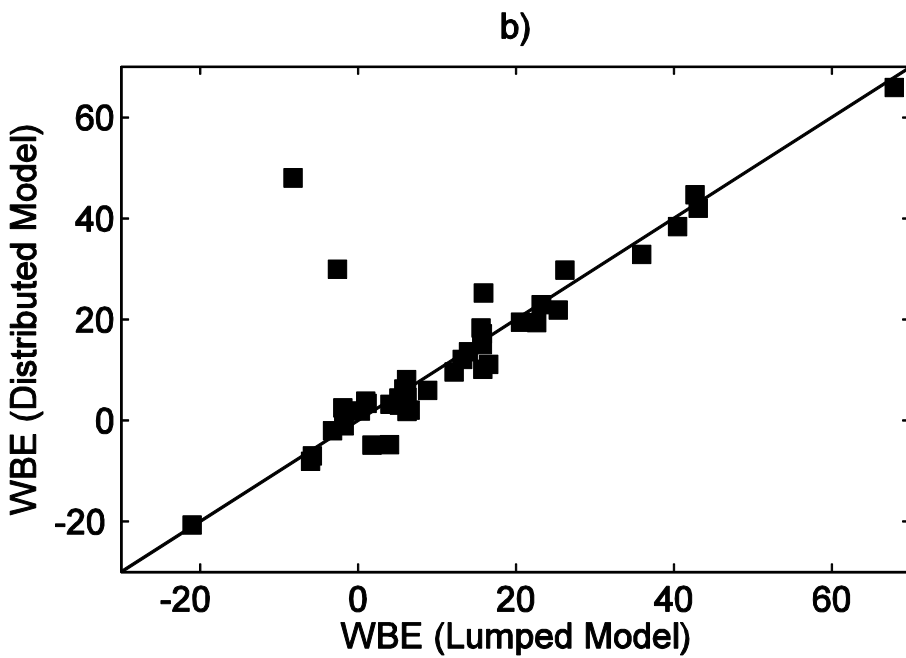
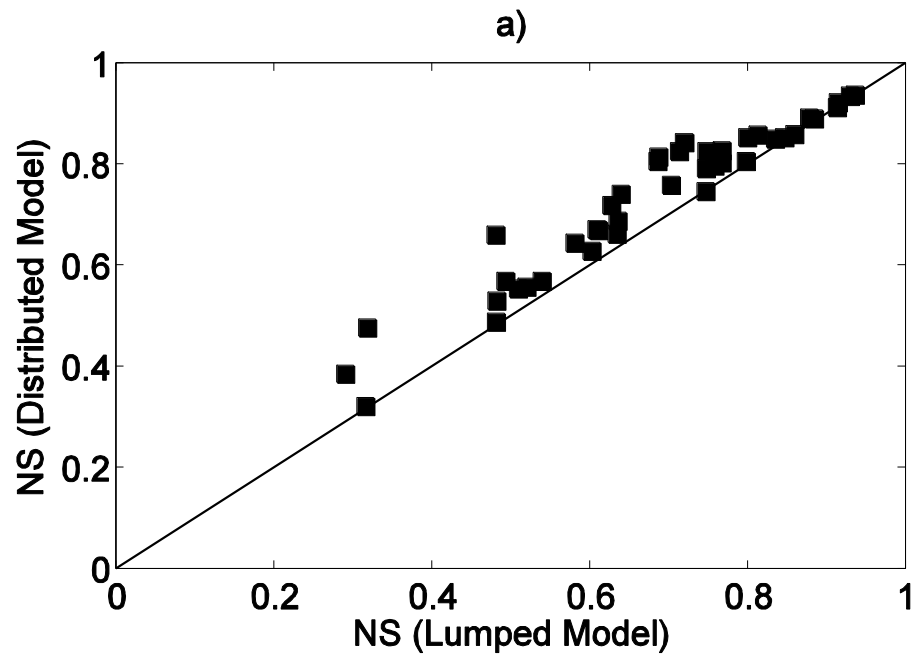
635



636

637 **Figure 3:** Representation of the individual landscape units within a catchment.

638

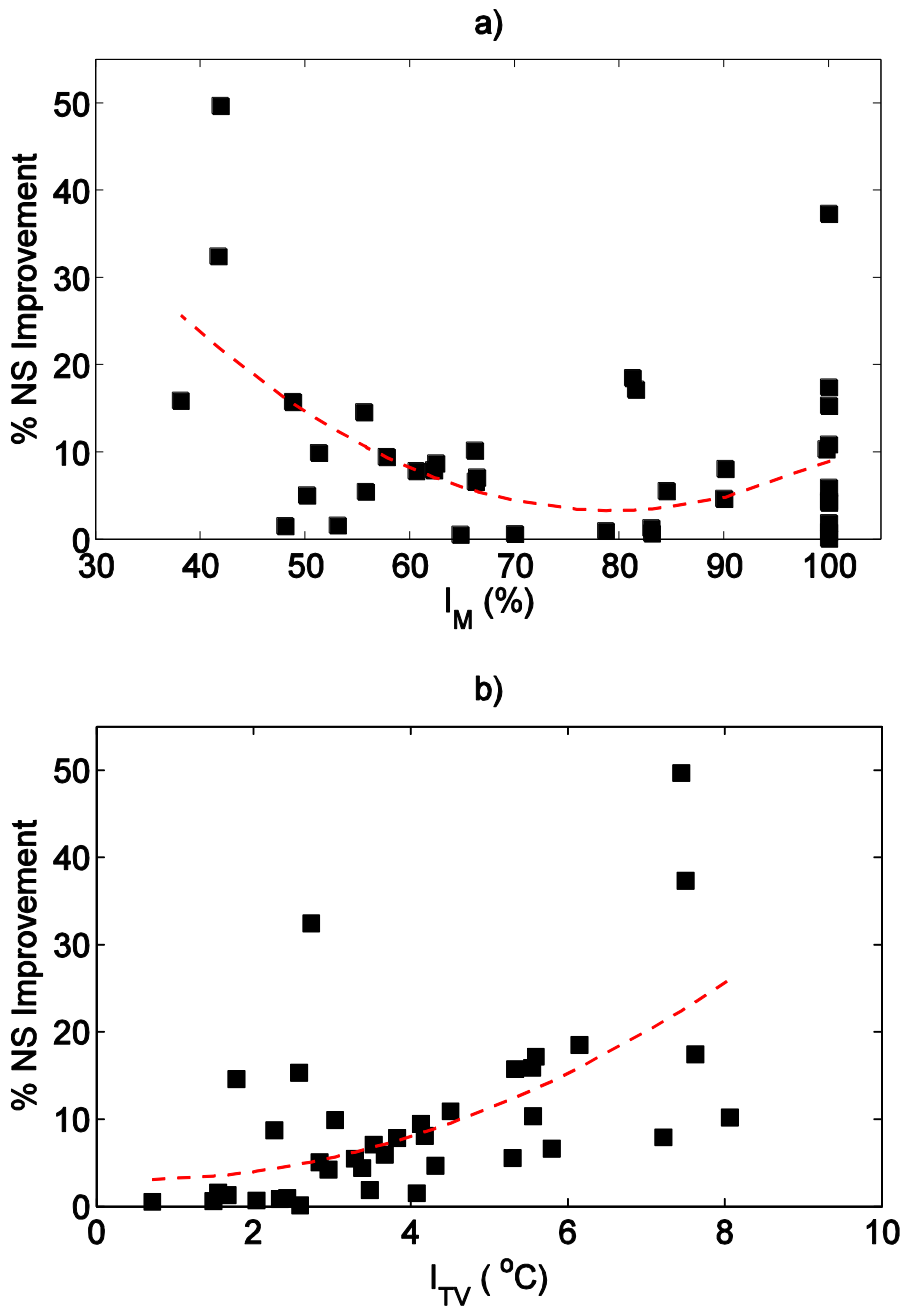


639

640 **Figure 4:** A one-on-one comparison between lumped and distributed EXP-HYDRO model with

641 a) Nash-Sutcliffe efficiency (NS), and b) Water Balance Error (WBE).

642

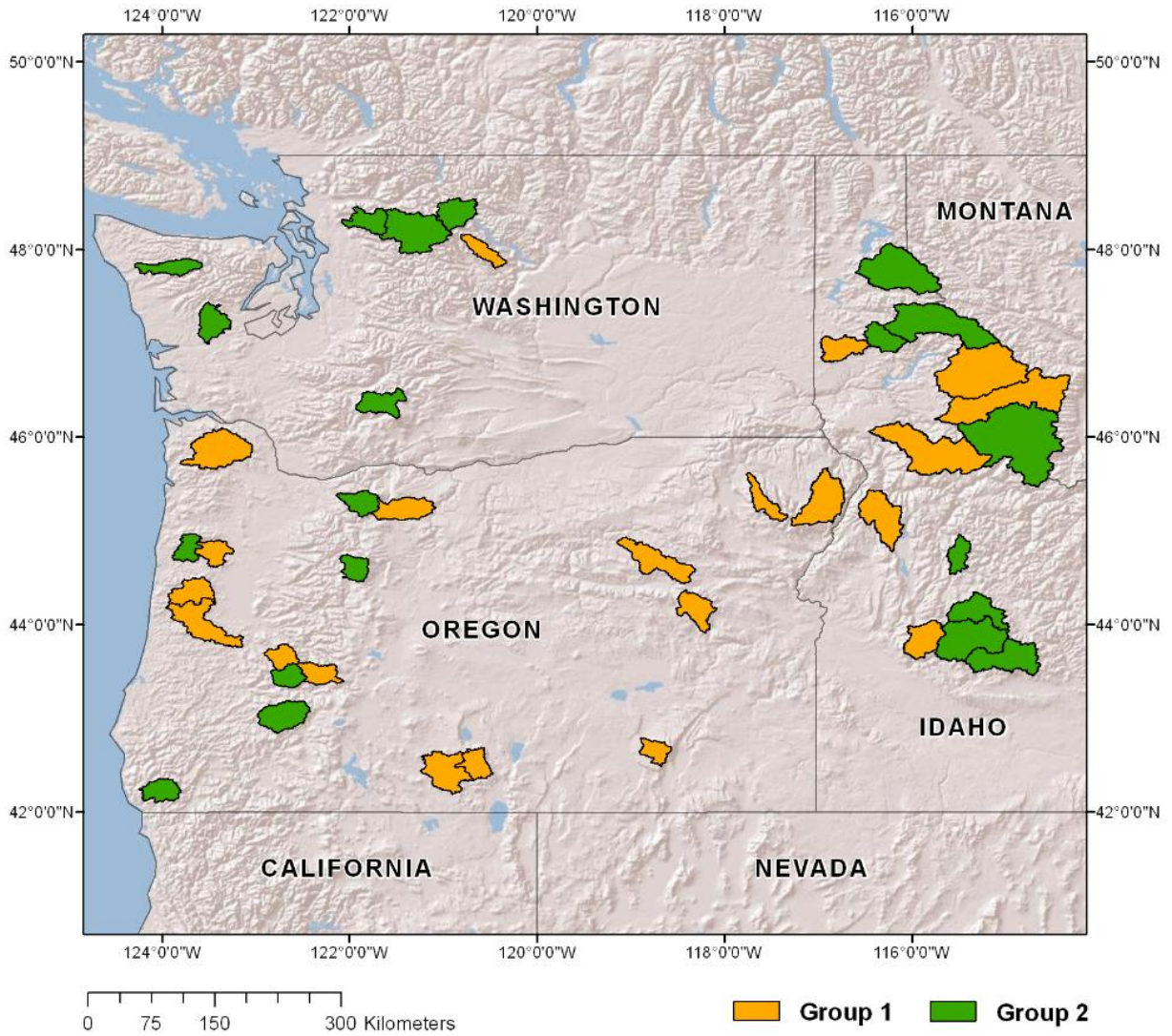


643

644 **Figure 5:** Relationship of model performance improvement with a) I_M , and b) I_{TV} . Red

645 dashed line is the regression fit using quadratic equation.

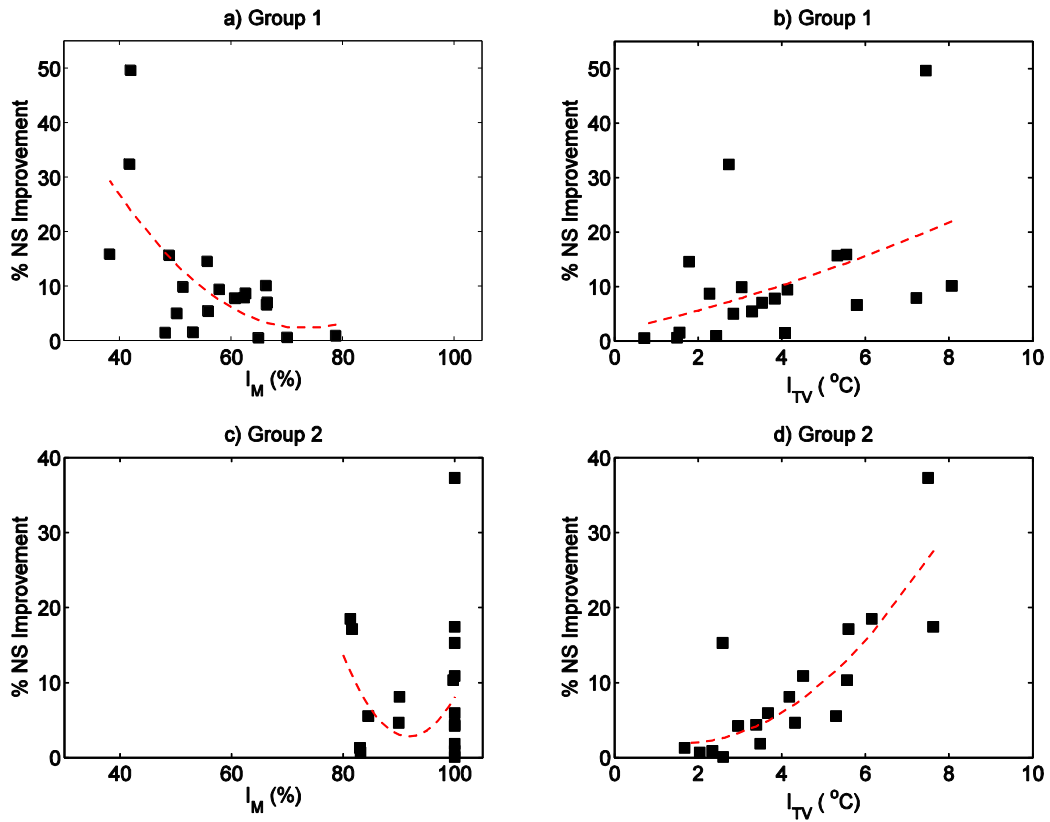
646



647

648 **Figure 6:** Location of the Group 1 ($I_M < 80\%$) and Group 2 ($I_M > 80\%$) catchments.

649



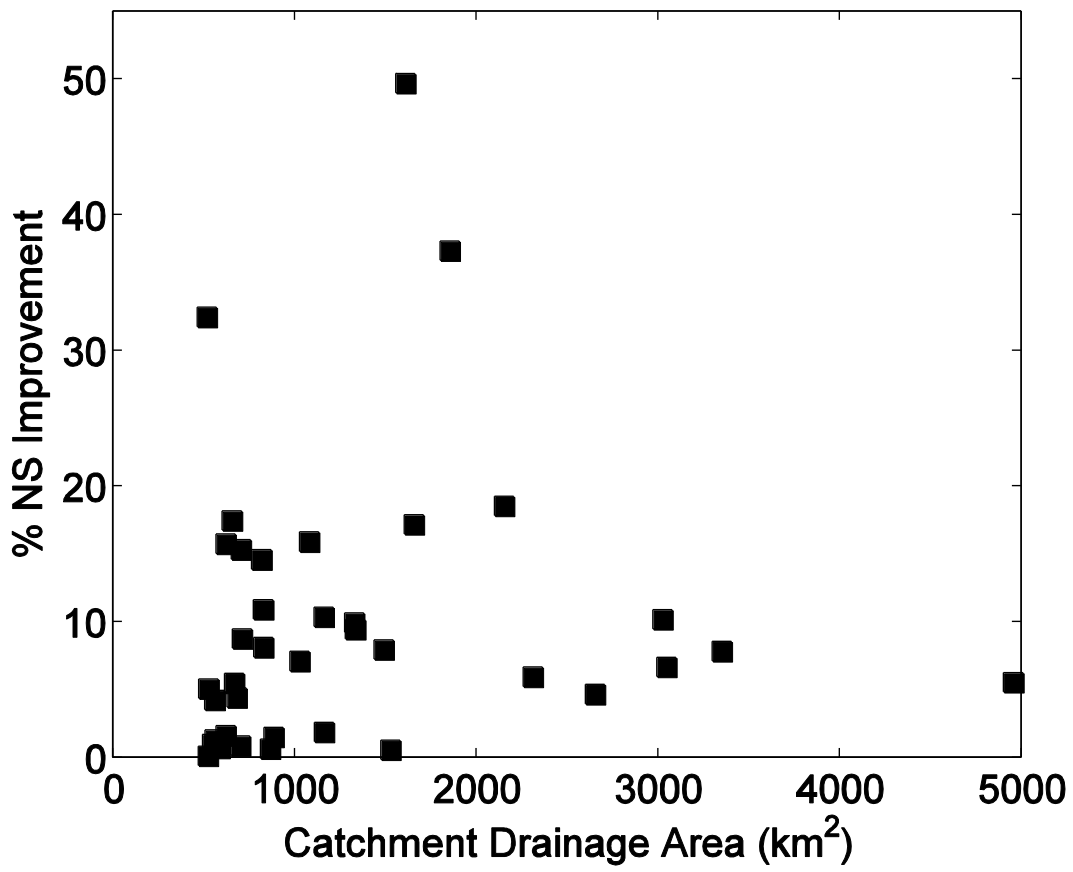
650

651 **Figure 7:** Relationship of model performance improvement with I_M and I_{TV} , shown separately

652 for the Group 1 and Group 2 catchments. Red dashed line is the regression fit using quadratic

653 equation.

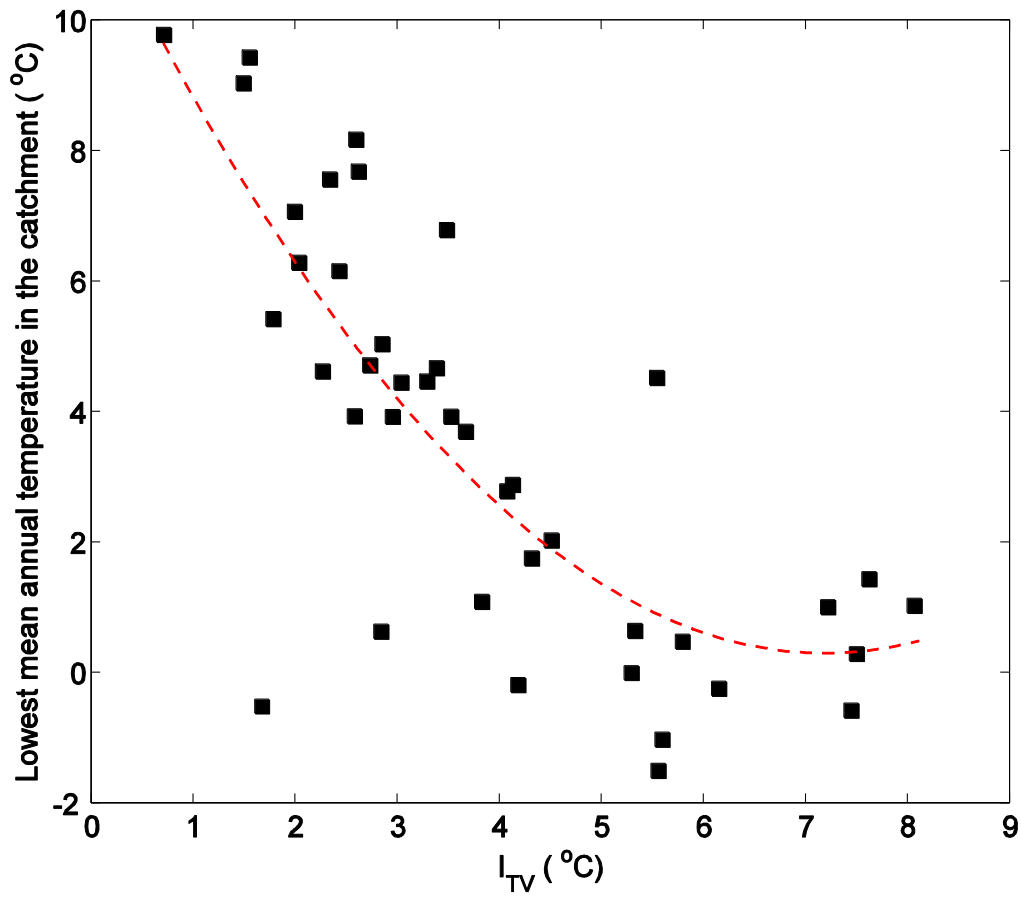
654



655

656 **Figure 8:** Relationship of model performance improvement with catchment drainage area.

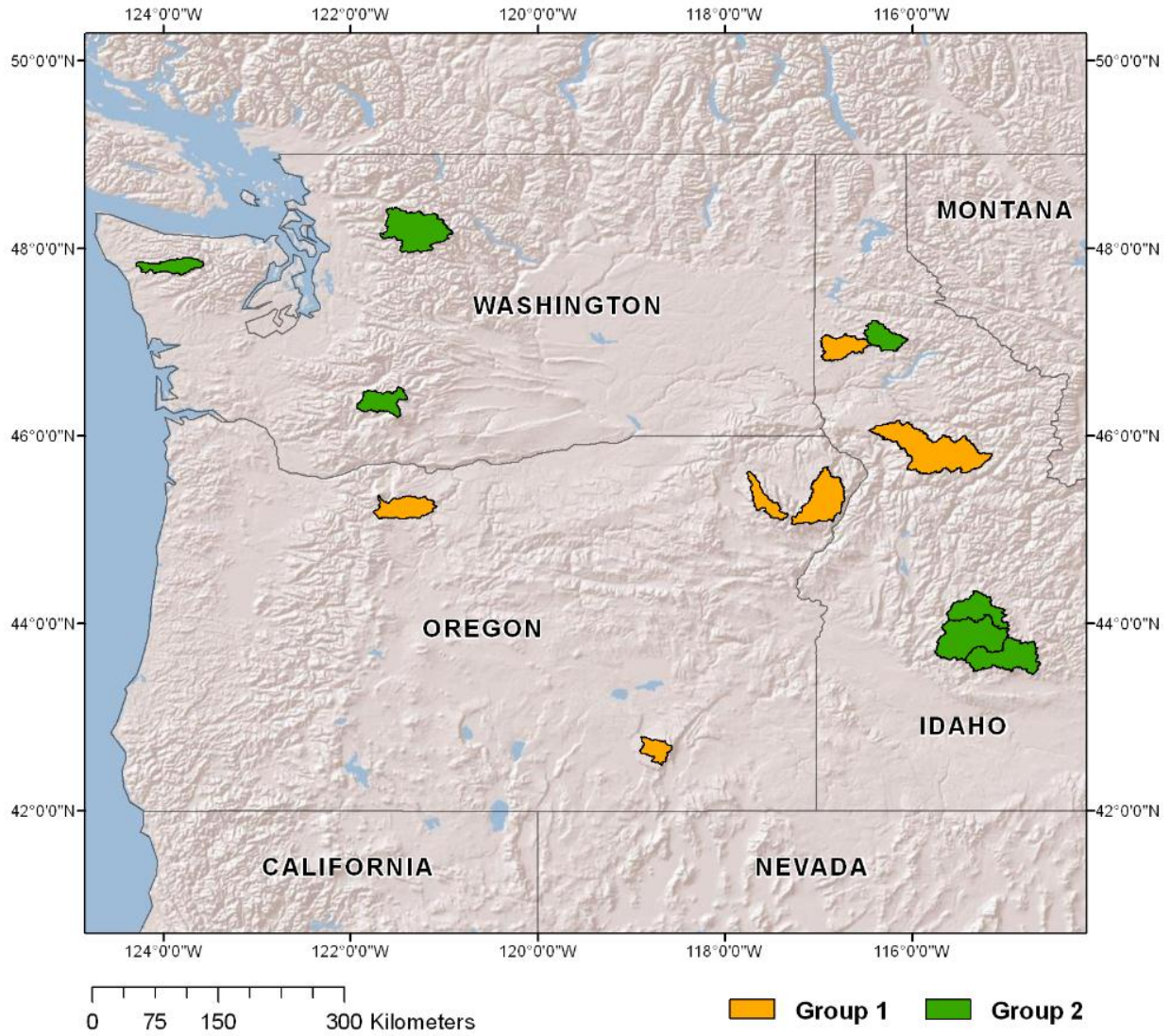
657



658

659 **Figure 9:** Relationship between I_{TV} and the lowest mean annual temperature within the
660 catchment. Red dashed line is the regression fit using quadratic equation.

661



662

663 **Figure 10:** Location of the catchments where distributed model shows more than 10% NS

664 improvement. Group 1 and Group 2 catchments are shown separately.